View metadata, citation and similar papers at core.ac.uk
brought to you by CORE
provided by NASA Technical Reports Server

POWDER BED FUSION ADDITIVE MANUFACTURING OF JBK-75

Z.C. Jones, P.R. Gradl
National Aeronautics and Space Administration
Marshall Space Flight Center
Huntsville, Alabama

ABSTRACT

JBK-75 is an iron-nickel derivative alloy of A-286 that has been of interest to NASA's propulsion community for use in fuel injectors and other components that are used in hot, corrosive environments. To enable the rapid production of these components in JBK-75, Marshall Space Flight Center has developed parameters for manufacturing fully dense JBK-75 components using powder bed fusion additive manufacturing (PBFAM). These parameters were developed in a two-step development. First, the depth of laser penetration in the powdered material was measured across a spectrum of laser powers to determine the optimal power necessary for generating the desired meltpool depth. The parameter set's vector-to-vector spacing was then then tailored to guarantee the full densification of the desired area. The results of this development was a readily implementable parameter that produced 99.6% dense material when using a 147W power running at 600mm/s with a 85µm(32%) vector-to-vector spacing.

INTRODUCTION

JBK-75 was first developed as a derivative alloy of A-286 that improved upon its predecessor's weldability as well as its hydrogen compatibility for use in applications that called for a precipitation hardened steel with high strength up to 922K (1,200°F) in both air and hydrogen. [1] As early as 1993, NASA began identifying JBK-75 as an alloy of interest in nozzles and fuel injectors. Drawbacks emerged in the implementation of JBK-75 in complex components, however, particularly in regards to machining it. The material's extreme abrasiveness resulted in a low tool life and a trade-off between chip control and surface finish [2], and thus an expensive and time-consuming machining operation.

In an effort to reduce the lead time and cost of JBK-75 parts, Marshall Space Flight Center (MSFC) began a project in 2018 to develop an additive manufacturing process for the alloy using a powder bed fusion process. The goal of the project was to prove the additive manufacturability of JBK-75 and produce a parameter set for PBFAM machines that allow for the production of fully dense components that require minimal machining or post processing.

Parameter sets are intrinsically necessary for an additive manufacturing process as contain the data that the machines use to coordinate the interdependent laser, focusing, and powder deliver systems that comprise the core of the platforms. Each alloy must have a parameter set developed for it, which is done by producing groups of samples made with different combinations of laser power, speed, and vector-to-vector spacing, also known as the hatch spacing, that together control the total energy input into the powder bed and thus how the powder is melted. [3] These samples are then cut and polished and analyzed either for the depth of the laser penetration or the density of the bulk material, at which point only parameters that produce the highest density continue to be developed by testing and verifying mechanical and microstructural properties.

It is a rarity for a single parameter set to be the one and only parameter set that a material can be run at. Instead, there is often a range of parameters within which a material can be successfully produced and which may allow you to prioritize certain elements of the production over others, i.e. a better surface finish may be achieved by running the laser slower, albeit at a cost of the component taking longer. [4] NASA's position in regards to this is to prioritize the density of the final part as the critical element of a parameter set with the speed of production being a secondary concern.

JBK-75 is primarily iron, nickel, and chromium with minor amounts of aluminum, titanium, and molybdenum and a melting point of 1672K (2.500°F). [5] The composition and melting point is most similar to Inconel 718 alloy that MSFC has extensive experience additively manufacturing

and analyzing, and so the initial starting points for the development were based on the current parameter set for Inconel 718, which runs at 180W, 600mm/s, and a hatch spacing of 105µm.

RESULTS AND DISCUSSION

EXPERIMENTAL

A ConceptLaser M1 PBFAM machine was used to manufacture the samples used in this project. This machine was chosen because it allowed for the complete editing of the parameters. There was a working familiarity with each parameter as well after having been extensively manipulated in previous developments of other alloys. The M1 had also been used exhaustively in the development of the Inconel 718 parameters that were used as the starting point, and so the machine and its idiosyncrasies were well known to the operators and engineering staff.

Concept Laser M1	
Version	2012 Model (Gen 1)
Build Capacity	250mm x 250mm x 275mm
Laser	Single 400W Nd:YAG
Spot Size	52µm
Laser travel Speed	50-5,000 mm/2
Inert Gas	Argon
Ventilator Flow	41%

Figure 1: ConceptLaser M1 Specifications

The recoating system for the M1 was fitted with a stainless steel blade for this development due to the need for strict control of the powder layer thickness to ensure that the later analysis for melt-pool penetration and density were correct and not subject to layer thickness variations. [6] The steel blade also eliminates the possibility for a test sample to warp upward and damage the recoater blade and cause a defect across the Y axis of a build, potentially causing a whole row of samples to be lost. Instead, should a test specimen fail in that manner the recoater blade will hit the sample, the torque limit on the recoating mechanism will be trigger, and the build will be paused and allow for the operator to cancel and remove the failing sample but continue with the remaining samples.

The sample geometry used in this project is a straightforward 25 x 10 x 19mm cube with 0.5mm fillets on the Z-axis edge and base cone that slopes at a 60° angle up to the full area. Cone bases are frequently used within NASA's AM lab to allow for test samples to be pulled off the build plate with pliers rather than having to be machined off, saving development time for the samples as well as reducing mundane machining operations to a minimum. The build plate itself was a standard 316L stainless steel build platen.

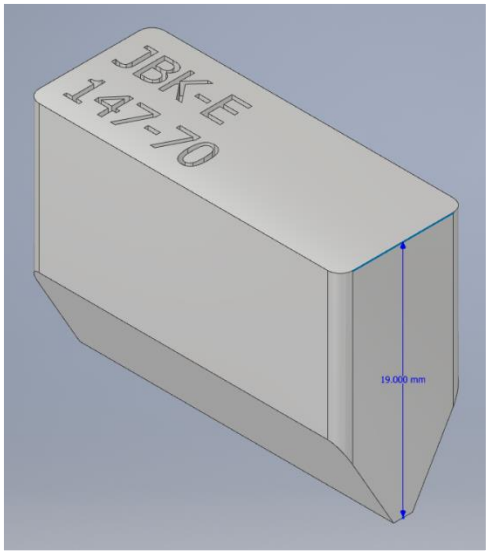

Figure 2: Sample geometry

Fifty-four total samples were initially produced in this development, with the samples being varied in both power and the hatch spacing but having a locked laser speed of 600mm/s. The layout and the labels are given in detail in figure 3. The variation in both hatch spacing and power allowed for the samples to serve both development goals simultaneously and reduce the number of sample cuts required. The samples at the highest range of vector-to-vector spacing could be used to measure the meltpool depth, which would then guide which power samples were analyzed, allowing for a very rapid development that required only 14 of the total samples to be sectioned.

The depth of the melt-pool is a critical element in a usable parameter set and a function of the

energy being put into the material by the laser. If the energy input in insufficient, the resultant melt-pool will be too shallow, fail to connect with the previous layers, and thus produce a defect-riddled part at best. [7] On the other hand, if the energy input is too high then the melt-pool will elongate, over penetrate into the previous layers, and form a deep melt-pool disrupted by the collapse of metal vapor pockets. The melt-pool then solidifies before it has the opportunity to stabilize and porosity is left by the perturbations. [8] The results of both these extremes is the same - a part with defects and porosity throughout the structure. For stainless steels and similar alloys, NASA's parameter sets target 2-4 layers of penetration, roughly 120-160µm from the top of the powder surface.

Once the power level needed to generate the ideal melt-pool depth is determined, the next element to determine is the hatch spacing. Hatch spacing is the distance between each pass of the laser as it rasterizes the part layer. Should the hatch spacing be too wide, the part will have visible gaps between each pass of the laser, resulting in a highly porous, low density part. Opposite of that, if the hatch spacing should be too close together then the vectors will overlap too much and the part will see too much heat input and develop the aforementioned turbulent melt-pool. While the exact hatch spacing is highly materially dependent, stainless steels have normally shown an optimal hatch spacing is in the range of 20- 40% of the melt-pool radius overlapping into the previous vector. [3]

Power (W)
147
155
163
171
181
190

Hatch Spacing (Label value - µm)
70 - 105 µm
67 - 100 µm
63 - 95 µm
60 - 90 µm
57 - 85 µm
54 - 81 µm
51 - 76 µm
49 - 73 µm
46 - 70 µm

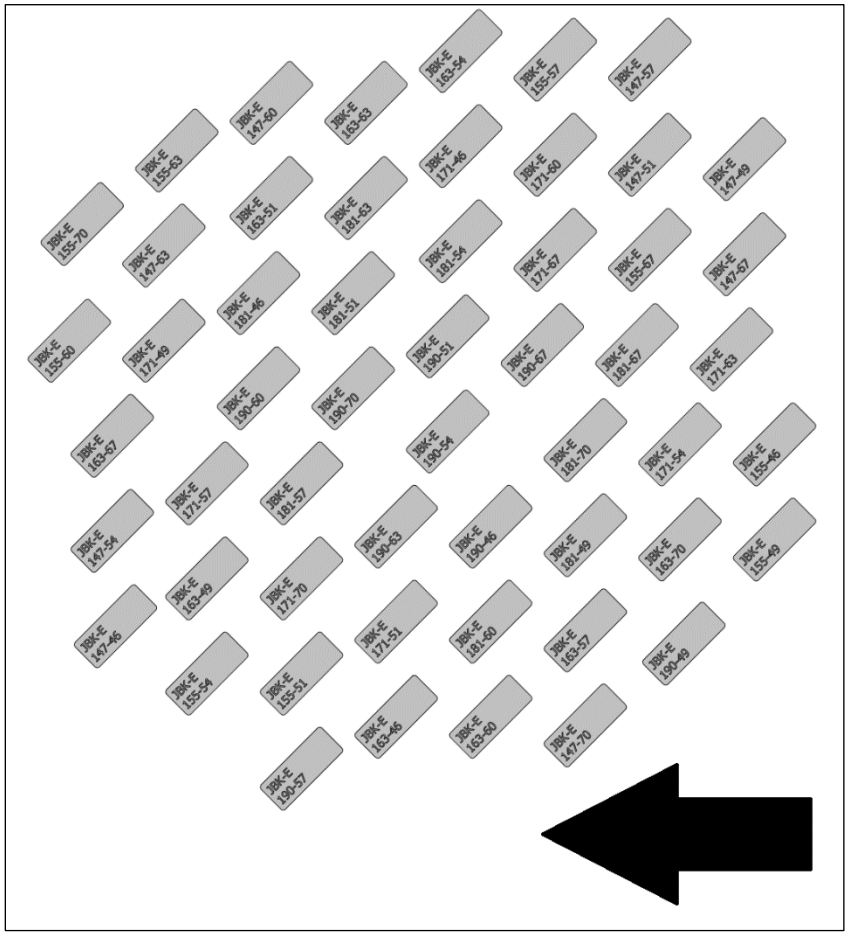

Figure 3: Sample build layout. Gas flow and recoating direction are denoted by the black arrow. Power level and hatch-spacing included in the tables to the left.

Samples were analyzed by first being cut by a cooled sectioning saw, hot mounted and polished. If the samples are being analyzed for melt-pool depth, they are then etched to reveal the individual melt-pools. If the samples are only being analyzed for hatch spacing then etching is not required as the hatch spacing will become evident in the porosity or lack thereof in the part.

The exact density of the part is then analyzed using threshold image analysis provided by the ImageJ2 program.

RESULTS

The samples at 105µm spacing were first cut and analyzed for melt-pool depth. It was immediately evident that the melt-pools were much deeper than anticipated. The range of depths seen was between 155um to 240um, whereas in Inconel 718 the comparable parameters would be generating depths that were half of that.

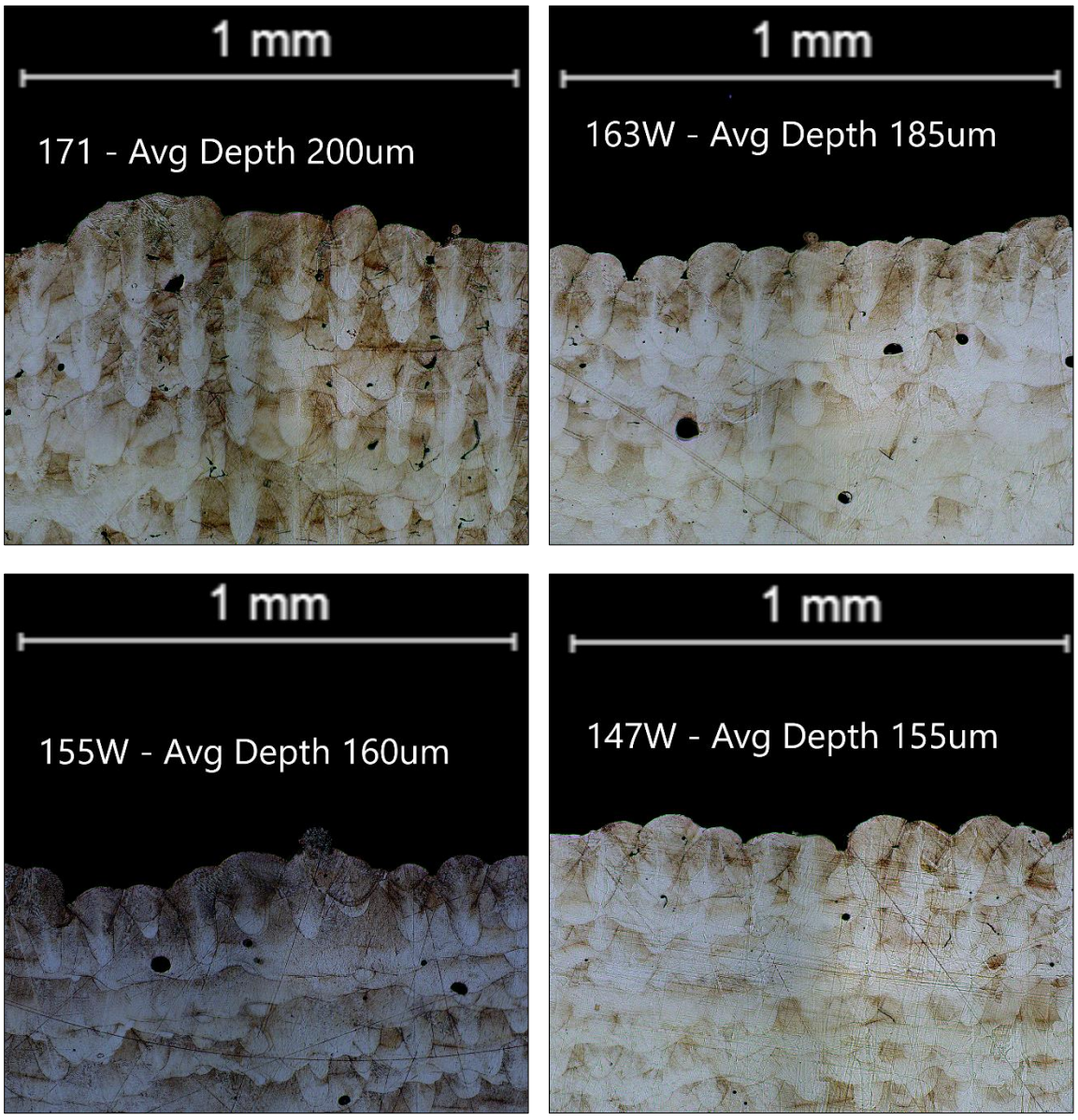

Figure 4: Etched samples and average calculated depths.

As can be seen in the pictures, the melt-pools are extremely deep and elongated in the at 171W, but decrease down to an acceptable 155um at 147W. While 155W is also in an acceptable range, 147 was ultimately the one that was chosen. At 147W the depths were more tightly grouped around 155 +- 15um as well as being more consistently ~125um in surface diameter.

Minimal elongation of the melt-pool was also seen at 147W, whereas 155 showed irregular elongation. These features combined created a highly predictable melt-pool that could be easily adjusted with hatch spacing to create a fully dense part.

The 147W power samples were then analyzed for density to determine the hatch spacing that provided the most fully dense bulk material. Most of the samples; density stayed well above 99.2%, although an ejecta-interference issue was discovered and will be discussed in the next section. The highest density was found at 147W – 85µm at 99.6%. This corresponds to a 32% overlap between the vectors.

Sample (Power(W) – Hatch Spacing(µm))	Density
147 - 100	99.33%
147 - 95	*97.91 *See next section on Ejecta Control.*
147 - 90	99.45%
147 - 85	99.68%
147 - 81	*93.95% *See next section on Ejecta Control.*
147 - 76	99.65%
147 - 73	99.62%
147 - 70	*89.78 *See next section on Ejecta Control.*

Figure 5: Densities of the 147W hatch spacing samples.

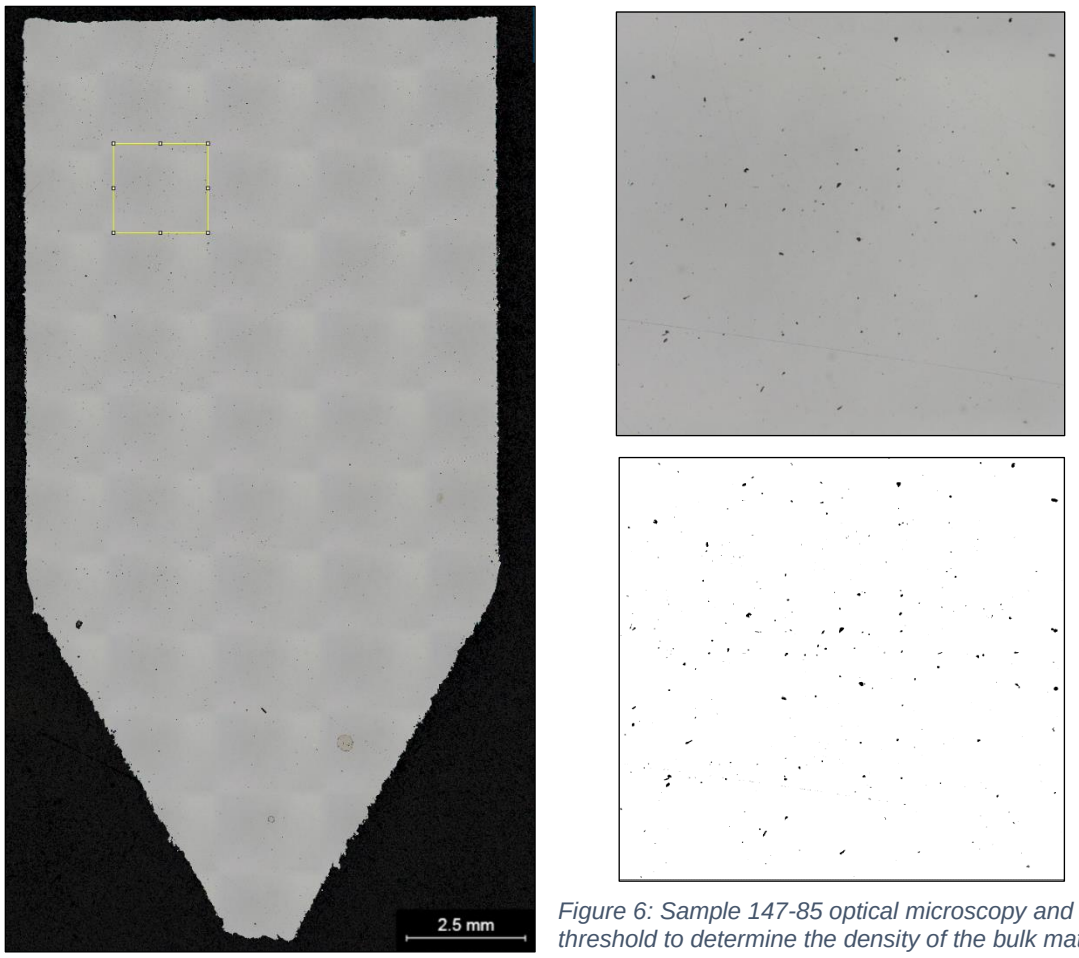

Figure 6: Sample 147-85 optical microscopy and image threshold to determine the density of the bulk material.

The porosity that was found was finely distributed across the part and did not congregate into specific areas or follow particular patterns. The average size of the pores was below <20µm with no pores being found to contain loose powder or partially sintered material to indicate that a

lack of fusion occurred. With the fully dense part well beyond the minimum density required to produce usable material, the parameters listed in figure 7 have been accepted as workable JBK parameters.

JBK-75 Parameter Set		
Power	Speed	Hatch Spacing
147 W	600 mm/s	85um

Figure 7: Final core parameters for JBK-75

EJECTA CONTROL

JBK-75 alloy produced significant amounts of ejecta during the build process, a well-known and documented phenomenon in the additive manufacturing process. The exact cause for this ejecta is a topic of debate and beyond the scope of this paper, however several samples of the JBK-75 showed massive degrees of porosity if they were directly in the ejecta path of a large number of parts. The current theory for why this porosity develops is that the misshapen ejecta particles cause small scale disruptions to the powder layering. As the powder layers are disrupted, the melt-pool becomes unstable and no longer fully fuses the powder, resulting in porosity. [9] The exact amount of ejecta falling onto a part to cause significant porosity is not yet know, but a mitigating laser scanning strategy was developed by MSFC. The strategy uses the laser to do a secondary, low power laser pass once all parts in a layer have been done to remove or melt accumulated ejecta from the exposed surface and allows for the fresh powder to successfully layer onto the part.

Pass Parameters	
Power	150W
Speed	2000mm/s
Hatch Spacing	105µm

Parameter Set	Without Cleaning Pass	With Cleaning Pass
147 - 95	97.91%	99.41%
147 - 81	93.95%	99.23%
147 - 70	89.78%	99.08%

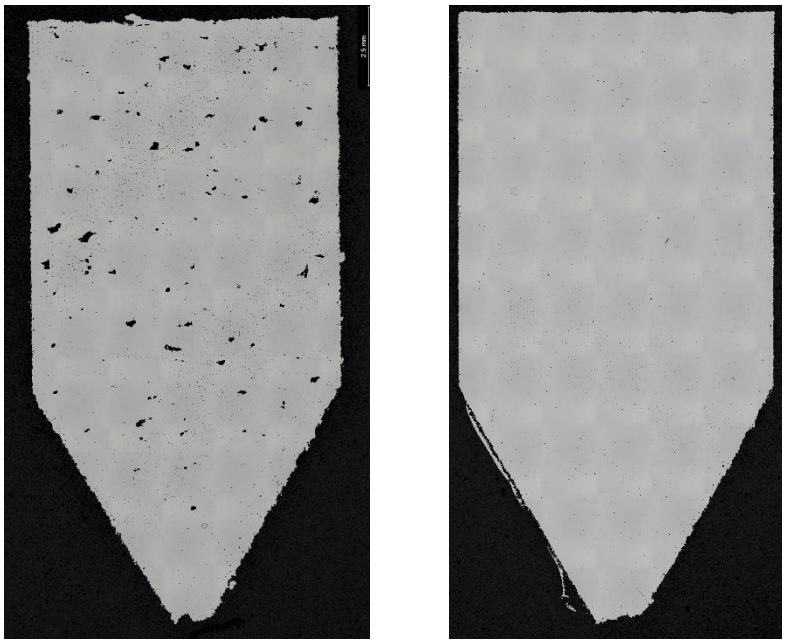

Figure 8: Sample 147-95 without cleaning pass (Left) and with cleaning pass (right).

SUMMARY AND CONCLUSIONS

JBK-75 has proven to be a readily usable alloy in PBFAM machines. Over the course of the development it has been shown to sustain a stable melt-pool as well as achieve an acceptable density of 99.6% across the bulk material without any secondary steps or processes being taken to further consolidate the material. In the event that significant ejecta should be noted in the build process, a prudent step to take at the current time is to implement the laser cleaning pass to clear the build surface of ejecta, however it is still highly recommended to take metallurgy samples and evaluate the density of the material in any build that sees significant ejecta.

FUTURE WORK

JBK-75 is an ongoing development process at MSFC and upcoming tasks include but are not limited to mechanical testing, the development of contour and support material parameters, verifying that traditional JBK-75 heat treatments are equally successful with additively manufactured JBK-75, and further investigation of the powder-ejecta interactions. MSFC will also soon begin the development of HR-1 alloy, a NASA developed derivative alloy of JBK that surpasses its predecessor in hydrogen compatibility.

ACKNOWLEDGEMENTS

Thank you to all the NASA personnel and contractors that worked on this project, in particular Ken Cooper, Paul Gradl, Ian Hanson, Colton Katsarelis, and Megan le Corre.

References

[1] A. Pandey, S. Shah, M. Shadoan and G. Lyles, "Selection and Evaluation of an Alloy for Nozzle Application," National Aeronatics and Space Administration, Huntsville, Alabama, 2003.

[2] A. P. McManigle and A. Simonis, "JBK-75 Stainless Steel Machinability Study," U.S. Department of Energy, Golden, Colorado, 1993.

[3] H. Gu, H. Gong, D. Pal, K. Rafi, T. Starr and B. Stucker, "Influences of energy density on porosity and microstructure of selective laser melted 17-4PH stainless steel.," in *Solid Freeform Fabrication Symposium V. 474*, 2013.

[4] K. Kempen, L. Thijs, E. Yasa, M. Badrossamay, W. Verheecke and J. P. & Kruth, "Process Optimization and Microstructural Analysis for Selective Laser Melting of AlSi10Mg," *Solid Freeform Fabrication Symposium,* vol. 22, pp. 484-495, 2011.

[5] SAE International, "Steel, Corrosion and Heat Resistant, Welding Wire 15Cr-30Ni-1.2Mo-2.2Ti-0.25Al-0.001B-0.030V ().1-0.03C) Vacuum Induction Melted, Environment Controlled Packaging. AMS5811E.".

[6] C. Meier, R. Weissbach, J. Weinberg, W. A. Wall and A. J. & Hart, "Critical influences of particle size and adhesion on the powder layer uniformity in metal additive manufacturing.," *Journal of Materials Processing Technology,* no. 266, pp. 484-501, 2019.

[7] J. P. Kruth, G. Levy, F. Klocke and T. H. C. Childs, "Consolidation phenomena in laser and powder-bed based layered manufacturing.," *CIRP annals,* vol. 2, no. 56, pp. 730-759, 2007.

[8] W. E. King, H. D. Barth, V. M. Castillo, G. F. Gallegos, J. W. Gibbs, D. E. Hahn and A. M. Rubenchik, "Observation of keyhole-mode laser melting in laser powder-bed fusion additive manufacturing.," *Journal of Materials Processing Technology,* no. 214, pp. 2915-2925, 2014.

[9] A. R. Nassar, M. A. Gundermann, E. W. Reutzel, P. Guerrier, M. H. Krane and M. J. Weldon, " Formation processes for large ejecta and interactions with melt pool formation in powder bed fusion additive manufacturing.," *Scientific reports,* vol. 1, no. 9, p. 5038, 2019.

[10] C. S. Marchi, "Technical Reference on Hydrogen Compatibility of Materials, Austenitic Stainless Steels: A-286(Code 2301)," U.S. Department of Energy, Livermore, California, 2005.

[11] I. Yadroitsev, A. Gusarov, I. Yadroitsava and I. & Smurov, "Single track formation in selective laser melting of metal powders.," *Journal of Materials Processing Technology,* no. 12, pp. 1624-1631, 2010.

[12] M. Xia, D. Gu, G. Yu, D. Dai, H. Chen and Q. Shi, "Influence of hatch spacing on heat and mass transfer, thermodynamics and laser processability during additive manufacturing of Inconel 718 alloy.," *International Journal of Machine Tools and Manufacture,* no. 109, pp. 147-157, 2016.